NANO LETTERS

Letter

pubs.acs.org/NanoLett

Dynamic Inversion Enables External Magnets To Concentrate Ferromagnetic Rods to a Central Target

A. Nacev,*[,†] I. N. Weinberg,[†] P. Y. Stepanov,[†] S. Kupfer,[†] L. O. Mair,[†] M. G. Urdaneta,[†] M. Shimoji,[†] S. T. Fricke,[‡] and B. Shapiro[§]

[†]Weinberg Medical Physics LLC, 5611 Roosevelt St, Bethesda, Maryland 20817, United States

[‡]Children's National Medical Center, 11 Michigan Ave NW, Washington, DC, 20010, United States

[§]Fischell Department of Bioengineering and the Institute for Systems Research, University of Maryland, College Park, Maryland 20742, United States

S *Supporting Information*

ABSTRACT: The ability to use magnets external to the body to focus therapy to deep tissue targets has remained an elusive goal in magnetic drug targeting. Researchers have hitherto been able to manipulate magnetic nanotherapeutics in vivo with nearby magnets but have remained unable to focus these therapies to targets deep within the body using magnets external to the body. One of the factors that has made focusing of therapy to central targets between magnets challenging is Samuel Earnshaw's theorem as applied to Maxwell's equations. These mathematical formulations imply that external static magnets cannot create a stable potential energy well between them. We posited that fast magnetic pulses could act on ferromagnetic rods before they could realign with the magnetic field. Mathematically, this is equivalent to reversing the sign of the potential energy term in Earnshaw's theorem, thus enabling a quasi-static stable trap between magnets. With in vitro experiments, we demonstrated that quick, shaped magnetic pulses can be successfully used to create inward pointing magnetic forces that, on average, enable external magnets to concentrate ferromagnetic rods to a central location.

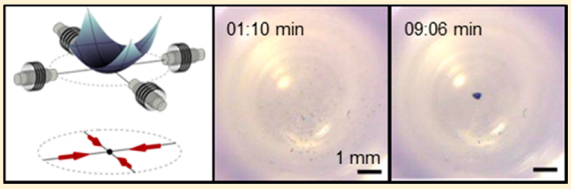

KEYWORDS: *Magnetic targeting, deep targeting, nanoparticles, concentrating magnetic nanoparticles, ferromagnetic rods, pulsed magnetic fields, Earnshaw's theorem*

The ability to deliver a therapy to any desired location within the body has been a primary goal of nanotherapy since its inception.[1] One way to achieve delivery of therapy to locations within the body is through the use of magnetic drug targeting.[2−9] To date magnetic targeting has been restricted to either using external magnets to focus therapy to shallow targets[2−7,10−12] or to implanting magnetic materials into the body in order to reach deeper targets.[13−15] In the first human trials for magnetic targeting, Lübbe et al.[3,16] used magnets to treat patients with superficial tumors. In recent years, researchers have implanted magnets or magnetizable materials at target locations in order to achieve greater precision in delivering therapies to treat parts of the body such as blood vessels[17,18] or the retina.[15] However, magnetic implants are not feasible for every biological condition and are not viable for every patient due to the need for additional procedures to place the magnets.[19] As a result, the scope and use of magnetic targeting has remained limited[20−25] when attempting to focus therapies to areas deep within the body using external magnets.

The difficulty of magnetic focusing to central targets between magnets follows in part from Samuel Earnshaw's 1842 theorem.[26] This theorem implies that no arrangement of static external magnets can magnetically focus therapy to a central target between the magnets.[20−25,27] When this theorem, which holds for any force field governed by an inverse squared law, is applied to magnetic fields and particles, it states that the inherent "instability [of particles] cannot be removed by [any] arrangement" of magnets.[26] The theorem proves that the sign of the curvature of the magnetic potential energy cannot be positive (no stable energy well possible) for spherical particles in a static magnetic field. Inspired by this theorem, we posited that by using ferromagnetic rods and fast magnetic pulses we could transiently reverse the sign of the potential energy and therefore enable a stable trap between magnets. The in vitro experiments below demonstrate that sequential magnetic pulses can focus ferromagnetic rods to a central target between magnets. We recognize that much work will be required to translate the results from an open vial of aqueous solution to complex biological systems that may include pulsatile flow and interfacial issues. A mitigating factor is that the above results were obtained with very low magnetic fields, as compared to the Tesla-level magnitudes that have been shown to be safe in humans,[28] and which would exert much more force on particles than in the above-described experiments. We hope that the results of this project will encourage investigators in the magnetic drug targeting field to pursue further research in

Received: September 23, 2014
Revised: November 30, 2014

dx.doi.org/10.1021/nl503654t | *Nano Lett.* XXXX, XXX, XXX−XXX

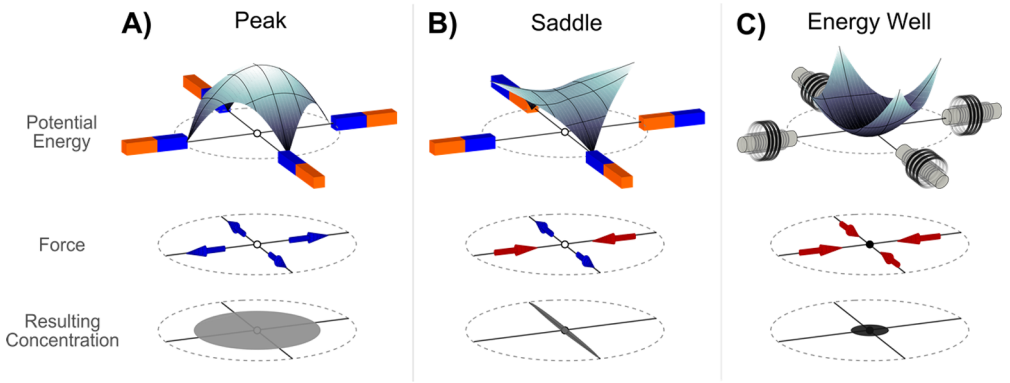

Figure 1. How forces generated from a magnet configuration affect particle concentrations. A magnet configuration creates a magnetic potential energy surface (top row) that generates the magnetic forces. Magnetic forces (middle row) shape particle concentrations (bottom row). Particles will move from locations of high-energy states (white) to low-energy locations (black). Equivalently, particles will move due to either divergent forces (blue arrows) or convergent forces (red arrows). By applying Earnshaw's theorem to static magnetic fields, only unstable static magnetic potential energy configurations were theorized to be possible, e.g., (A) a peak energy configuration and (B) a saddle. (C) Through the use of pulsed magnetic fields, we have achieved the creation of a magnetic potential energy well on-average that is capable of concentrating particles to a central target.

shaped magnetic fields and in particle designs in order to eventually achieve clinical translation.

Exploiting Magnetic Relaxation to Focus Particles. The mathematics covered by Earnshaw's theorem[26,27,29,30] are based on a system where magnetic materials are attracted to each other by a force that is inversely proportional to the distance squared between them. For such a situation, Earnshaw's theorem states that the Laplacian of a magnetic particle's potential energy in the applied magnetic field is at best equal to zero ($\nabla^2 U = d_x^2 U + d_y^2 U + d_z^2 U = 0$). Thus, the curvature of the potential energy for any particle at any location cannot be positive ($\nabla^2 U$ cannot be greater than 0) and so Earnshaw's theorem states that it is not possible to form a stable equilibrium (an energy well) between magnets. In Earnshaw's words, with parenthetical text added for clarity: "It may be observed also that the instability cannot be removed by arrangement [of the particles or external magnets] for though the values of $d_x^2 U$, $d_y^2 U$, $d_z^2 U$ depend upon the arrangement of the particles, the fact that one at least must be positive and one negative depends only upon the equation $d_x^2 U + d_y^2 U + d_z^2 U = 0$ which is true for every arrangement."

Earnshaw's mathematical formulation has been applied to a magnetizable particle under the influence of a static magnetic field.[27] The potential energy of a magnetic particle is $U = -\mu_0 \mathbf{M}\cdot\mathbf{H}$, where the dot product of the particle magnetization $\mathbf{M}$ and the applied magnetic field $\mathbf{H}$ is multiplied by the permeability of free space μ_0. Without magnetic saturation, the particle magnetization is $\mathbf{M} = \chi V \mathbf{H}$, where the magnetic field is multiplied by the material magnetic volume susceptibility and the particle volume. In other words, the potential energy of the particle is determined by the particle's magnetization alignment with the external magnetic field. Typically, small particles align with the magnetic field first *before* moving along the magnetic field gradient. By using Maxwell's magnetostatic equations, it can be shown that the energy of a small particle that has undergone such an alignment is $\nabla^2 U = -\kappa(|\nabla H_x|^2 + |\nabla H_y|^2 + |\nabla H_z|^2)$, where $\kappa = \mu_0 \chi V$. Since the elements within the parentheses are always positive, and since κ is always positive for ferri-, ferro-, or paramagnetic particles, the resulting system is unstable (the curvature of the magnetic potential energy can never be positive: $\nabla^2 U \leq 0$). In the case of diamagnetic materials (e.g., water, pyrolytic graphite), κ is negative. However, the magnetic constants of diamagnetic materials are orders of magnitude smaller than for ferromagnetic materials, implying that extremely strong magnetic fields and magnetic field gradients are required in order to push or concentrate diamagnetic materials.

The instability stated in Earnshaw's theorem implies that a distribution of particles can never be focused to a central target by using external *static* magnets. This implication has been cited by investigators in the field of magnetic particle therapeutics as a major challenge.[21,31] Figure 1 illustrates how various potential energy shapes impact a distribution of ferri-, ferro-, or paramagnetic particles. Under the $\nabla^2 U \leq 0$ curvature constraint stated by Earnshaw, magnetic field configurations can be made to generate magnetic forces that spread particles out by creating a magnetic energy peak (Figure 1A). Alternatively, a magnetic energy saddle point can be made that generates magnetic forces pushing particles together in one direction, but as described by Earnshaw's theorem, this saddle point will also create forces spreading the particles out in another direction (Figure 1B). To date, there has been no demonstration of how to create a magnetic energy well that generates forces capable of focusing all particles to a central location (Figure 1C). If such a magnetic energy well was generated, it is possible that it could be used to focus particles to a central target deep within the body.

If we no longer consider the case of static magnetic fields and instead broaden our consideration to include the possibility of transient magnetic fields, then it becomes possible to choose a magnetic field configuration that can focus magnetic materials to a central target. If instead of using spherical particles we use rods, which align with the magnetic field only *after* they have already begun moving along the magnetic field gradient, we can effectively reverse the sign in Earnshaw's curvature constraint and achieve an energy well (a stable equilibrium).

In this work, we experimentally show in vitro that, by quickly pulsing magnetic fields, ferromagnetic rods can be forced to temporarily invert their magnetic potential energy shape, thereby concentrating an arbitrary number of ferromagnetic rods to a central target. Rods have been shown by previous reports to have in vitro and in vivo efficacy of nanorod-based gene delivery.[32] We are currently working to demonstrate our approach in vivo, and also to show the safety of our method, and those results will be reported in future publications. If successful, combined with clinically available magnetic fields and gradients,[27,33−35] this method opens the possibility of

dx.doi.org/10.1021/nl503654t | *Nano Lett.* XXXX, XXX, XXX−XXX

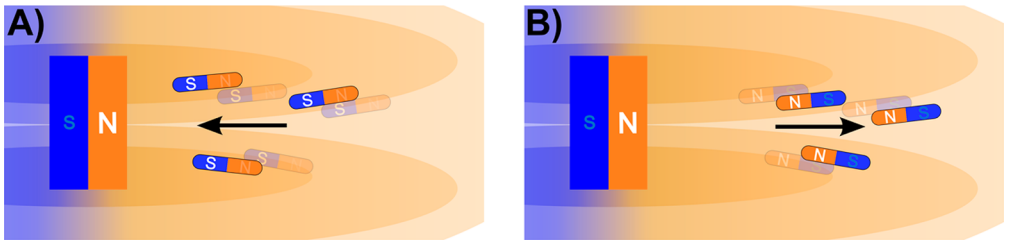

Figure 2. Movement of small ferromagnetic rods in response to a magnet. (A) When the rods are aligned with the magnet (e.g., the north pole of the magnet near to the south poles of the rods), then the rods are attracted to the magnet. (B) When the rods are antialigned with the magnet (e.g., north poles of the magnet near to the north pole of the rods), then the rods are pushed away from the magnet.

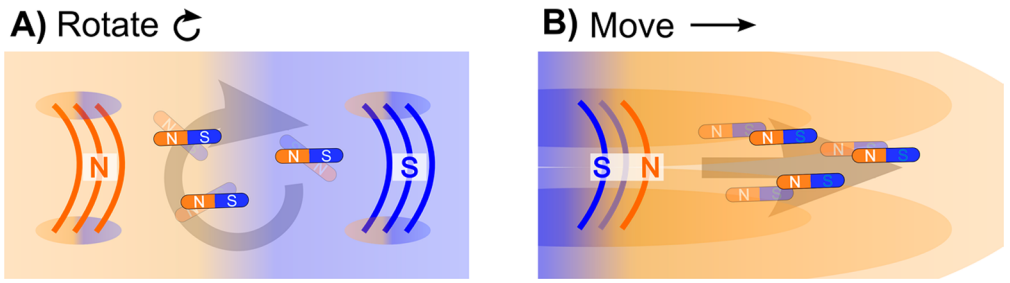

Figure 3. How we reverse the sign of Earnshaw's curvature constraint. (A) Using two electromagnets, a uniform magnetic field is applied that rotates the rods to match the field. (B) A gradient that is opposite in alignment from the rods is then applied causing the rods to move away from the magnet.

effectively delivering therapies to target areas deep within the body by using external magnets.

The Physics of Inverting Ferromagnetic Behavior. The main idea behind our technique can be conceptualized by observing the behaviors of toy bar magnets. At short time scales, small ferromagnetic rods act as tiny bar magnets. When these small rods are near a large magnet, the rods' poles closest to the magnet will determine the rods' behavior (see Figure 2). In one configuration, if the poles of the rods nearest the magnet are opposite, then the rods will be attracted toward the magnet (Figure 2A). In another configuration, if the poles closest to each other are the same, then the magnet will repel or push the rods away (Figure 2B). Regardless of whether the rods are being attracted or repelled, the magnet is simultaneously rotating the rods so that the rods' closest poles will be opposite to the magnet's closest pole. Therefore, given enough time, the rods will *always* be pulled inward toward the magnet.

Our technique capitalizes on the ability of magnets to repel ferromagnetic rods that are antialigned with the magnet (Figure 2B). Specifically, our technique has first been applied to ferromagnetic rods due to their stabilized magnetic domains, which allows their behavior to more closely resemble the behavior of tiny bar magnets. We first apply a uniform magnetic field that orients the rods in one direction. We then apply a magnetic field gradient that is antialigned with the rods (e.g., the closest pole of the magnet matches the closest pole of the rod) so as to ensure the initial movement of the rods is away from the magnet. Mathematically, the potential energy ($U = -\mu_0 \mathbf{M}\cdot\mathbf{H}$) of such antialigned rods will be *inverted* since the rod magnetization is now opposite that of the magnetic field (e.g., $\mathbf{M}/\|\mathbf{M}\| = -\mathbf{H}/\|\mathbf{H}\|$). This type of inversion ultimately allows for the creation of a magnetic energy well, as the Laplacian of the magnetic potential energy will now initially be greater than zero, $\nabla^2 U > 0$. Through this technique of dynamically inverting the magnetic forces, we attain well-like curvatures of magnetic potential energy surfaces.

The key technical component of our technique is to invert the magnetic potential energy by the exploitation of the rotational dynamics of the ferromagnetic rods. First, we apply a uniform magnetic field that polarizes the rods. This is accomplished by actuating two electromagnets around the rods to transiently generate a uniform polarizing magnetic field that rotates the rods so that the rods' alignment matches the magnetic field alignment (Figure 3A). This places the north poles of the rods to match to the north pole of the external field and the south poles of the rods to the south pole of the field. Since this uniform field has no spatial field gradient, it does not translate the rods. The uniform field is removed once the rods are aligned, at which time a transient gradient field (from only a single electromagnet) is applied that is antialigned with the polarizing field. Since the new gradient field is antialigned with the polarizing field, it is also antialigned with the rods' prior orientations. As a result, the rods will be repelled by this applied gradient field (Figure 3B).

The sequential application of two magnetic fields, one to polarize and the other to push, can momentarily repel rods away from a magnet. However, the rods can only be repelled while they remain *anti-aligned* with the gradient field. During the application of the transient gradient field, the rods will be repelled and will also begin to rotate to match the alignment of the gradient field. Once rods match the gradient field alignment, they will no longer be repelled and will begin to be attracted toward the magnet. Therefore, there exists a maximum time duration of the gradient field before rods eventually rotate their magnetization and are attracted to the electromagnet.

The transient repulsion described above (instead of the usual attraction of particles to magnets) switches the sign in Earnshaw's formulation. It converts $\nabla^2 U \leq 0$ to $\nabla^2 U \geq 0$ and allows the inversion of an energy peak (Figure 1A) into an energy well (Figure 1C). To achieve such an energy well on average, we use pulsed electromagnets arranged in two

dx.doi.org/10.1021/nl503654t | *Nano Lett.* XXXX, XXX, XXX−XXX

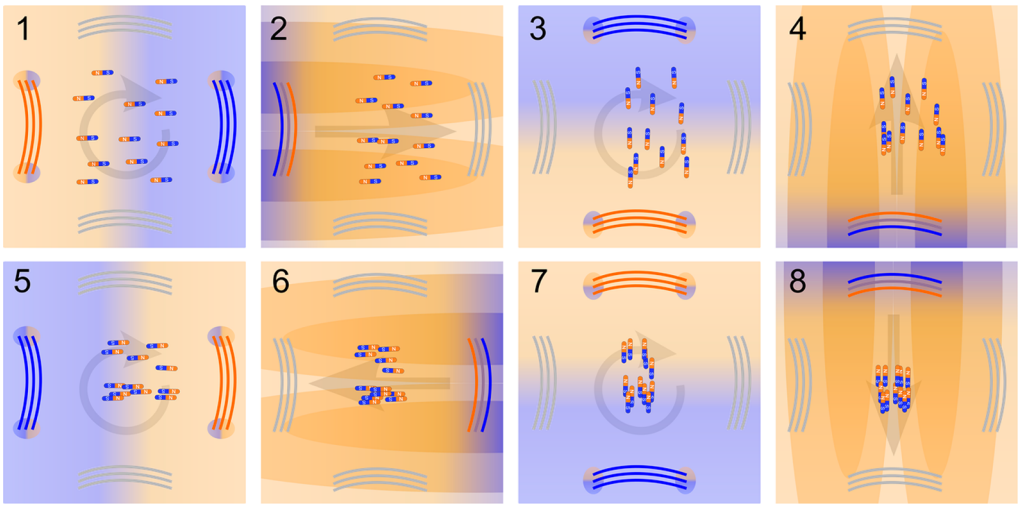

Figure 4. Sequence for creating a magnetic energy well. These 8 steps can be repeated multiple times to concentrate the ferromagnetic rods at a central location. The particles are (1) rotated to match a horizontal field, (2) repelled to the right, (3) rotated to match a vertical field, (4) repelled upward, (5) rotated to match a horizontal field, (6) repelled to the left, (7) rotated to match a vertical field, and then (8) repelled downward.

dimensions around a collection of ferromagnetic rods (see Figure 4). The sequence of activations shown in Figure 4 is designed to concentrate rods in two-dimensions by subsequently aligning and repelling rods in four directions. As each act of repulsion has a magnetic potential energy curvature greater than zero, the magnetic potential energy curvature on average will also be greater than zero, and an energy well will be formed. This sequence will therefore concentrate the rods to a central target. It follows that, by applying a repulsive force in both the positive and negative z direction, the rods can be focused in three dimensions.

To better understand the maximum allowable duty cycle of the repulsive gradient field, it is important to discuss the two types of effects behind the rotation of the magnetization of the rods: Brownian and Néel relaxation.[36−38] Brownian relaxation describes the alignment of a particles' magnetization with the field due to the physical rotation of the particles within the fluid. Néel relaxation describes the shifting of the particles' magnetic domains so that they match the external field. Usually, the hydrodynamic resistance for reorienting the particles in space is less than the magnetostatic resistance for reorienting the particles' poles (e.g., for ferromagnetic particles). Typically, small superparamagnetic particles have short Néel and Brownian relaxation times (<100 ns), while larger ferromagnetic and paramagnetic rods have much longer relaxation times >100 μs.[36−38] To achieve effective continuous repulsion of the ferromagnetic rods, the pulse duration of the magnetic gradient field should be less than the time it takes for the rods to realign with the gradient field. This is easier to achieve with rods compared to spheres, where the elongated shape of a rod grants the particles a higher moment of inertia. Under Brownian relaxation, cobalt rods (with a length of 200 μm, diameter of 200 nm, and a magnetic susceptibility of 0.65[39]) would take approximately 500 μs to rotate and match a perpendicular magnetic field of 0.5 T.[40] In the experiments described below, we applied the gradient field for 50 μs, which is a much shorter time than it takes the rods to rotate. Since the rod magnetization will be opposite to the gradient field during the time the transient gradient field is applied, the rods will be repulsed by each electromagnet. Consequently, the magnetic potential energy can be inverted and, therefore, allows for the rods to be focused.

Experimental Results. To demonstrate the dynamic magnetic inversion technique, we first built a system to push rods in one dimension. This system was used to confirm our hypothesis that the forces produced from the pulsed magnetic fields acting upon the ferromagnetic rods would indeed invert the magnetic potential energy shape. Both the one-dimensional and two-dimensional experiments are detailed in the Supporting Information. Next, we built a system to experimentally demonstrate that dynamic magnetic inversion could focus cobalt rods in two dimensions (2-D). The 2-D magnetic focusing experimental system consisted of two Helmholtz coils (square diameter of 5 cm with 44 turns per side powered by a maximum of 11 A) for polarizing the rods, four gradient coils (2 cm diameter coils, 2 cm in length, with 120 turns powered by a maximum of 66 A) for transiently repulsing the rods, a USB camera (Celestron model 44302-A) for optical visualization of the rods, and a custom-built system using high voltage relays (Gigavac GH1) that controlled which coils received current. All coils surrounded a 25 mm × 25 mm sample region (see Figure 5).

Cobalt rods (5 mg of 200 μm long × 200 nm, from PlasmaChem GmbH, Cat. Nr. PL-CoW200) were suspended within a 12 mm vial containing a 1:5 solution of hexane:isopropanol (solution used for reduced viscosity, however water can alternatively be used). The rods were dispersed by gently shaking the vial, making them initially undetectable to the unaided eye. The vial was placed within the sample region of the 2-D pulsed magnet system (Figure 5A). Last, we applied a train of magnetic pulse sequence elements shown in Figure 5B. Each pulse sequence element comprises the polarizing pulse followed by a short 5 μs delay time and finished with the gradient pulse. This pulse sequence element was repeated continuously and oscillated in all four directions ($+x$, $-x$, $+y$, and $-y$) as shown above in Figure 4. The applied sequence of magnetic fields and gradients concentrated the ferromagnetic rods tightly to the central target, as shown in the final panel of Figure 6. Focusing has also been demonstrated for custom grown 250 nm diameter nickel rods that are 2−8 μm in length and either without a coating or with a coating of 1 kDa

dx.doi.org/10.1021/nl503654t | Nano Lett. XXXX, XXX, XXX−XXX

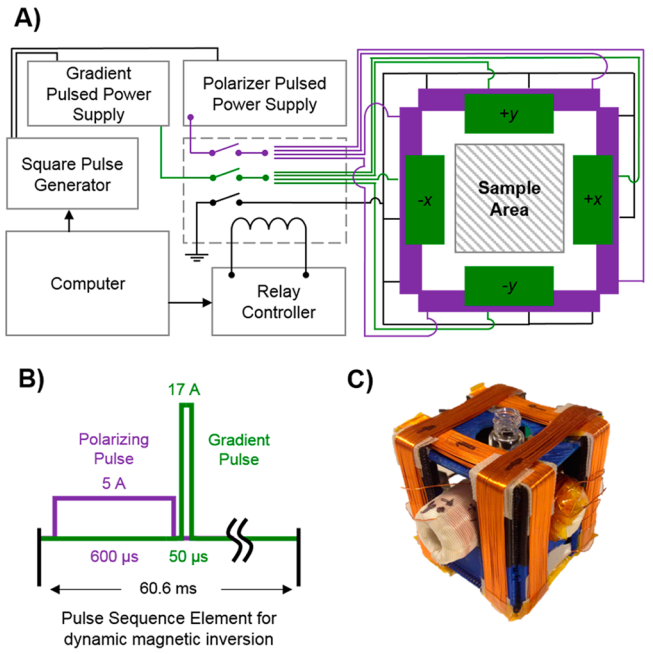

Figure 5. Experimental system for dynamic magnetic inversion that repulses and concentrates rods in two-dimensions. (A) Schematic showing a computer controlling both the square pulse signal generator and the relay controller. Pulsed power supplies provided current to the high voltage relays, which passed the current into a specified pair of coils. Any axis can therefore be polarized in any direction as dictated by the computer graphical user interface. (B) Pulse sequence element for inverting the energy surface of ferromagnetic rods and concentrating them at the center of the sample area. This pulse sequence element is repeated many times for the four directions to push and concentrate the rods to the center. The applied sequence of magnetic fields and gradients used to concentrate rods to the center is shown schematically in Figure 4. (C) Photograph of the wound coils surrounding the sample area.

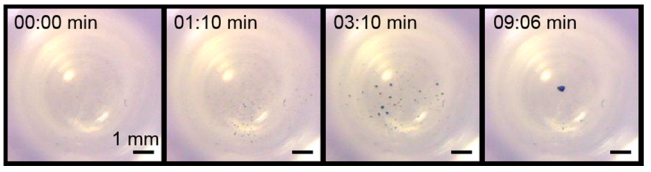

Figure 6. Focusing of ferromagnetic rods to a central target. Four snapshots of concentrating cobalt rods to the center of the sample area using dynamic magnetic inversion. The rods began optically undetectable and dispersed throughout the region. After 09:06 min, the rods were concentrated at the center of the sample area. Video available as Supporting Information.

PEG. Focusing has been accomplished for all particle types in three solutions: a 1:5 hexane to isopropanol solution; tap water; and 1× phosphate buffered saline (Sigma Aldrich).

The experiment results shown in Figure 6 illustrate that pulsed magnetic focusing worked in vitro. Development of the method for safe and effective operation in vivo is the subject of ongoing work and will be reported in future publications.

Conclusion. Magnetic forces have been used to manipulate therapies in human patients, but the scope and utility of magnetic targeting using external magnets has been limited to superficial targets. We have shown in vitro that pulsed magnetic fields can exploit the rotational dynamics of ferromagnetic rods and thus attain well-like curvature of the magnetic potential energy. By applying transient magnetic gradients before the rods have had an opportunity to realign with the magnetic field, we can reverse the direction of forces and can create a stable energy well (i.e., inward pointing magnetic forces). Using this approach, we focused a disperse concentration of ferromagnetic rods to a central target between eight external electromagnets. In future work, we hope to demonstrate pulsed focusing to central targets between magnets in vivo, to validate safety, and to scale-up the method to the distances anticipated in human patients. Success would grant clinicians a tool capable of delivering therapy where it is needed, a key goal in magnetic drug targeting.

■ ASSOCIATED CONTENT

Supporting Information

Details of the experimental set-ups for the one-dimensional and two-dimensional systems, as well as the results. In addition, a video for Figure 6 is available. This material is available free of charge via the Internet at http://pubs.acs.org.

■ AUTHOR INFORMATION

Corresponding Author

*E-mail: alek@nacev.me.

Notes

The authors declare no competing financial interest.

■ ACKNOWLEDGMENTS

Funding from the National Institutes of Health (NIH, grant numbers 1R21CA140068-01, 1R41DC013534-01A1, 1R43CA174280, and 5R42NS073289) and the National Science Foundation (NSF, grant number NSF 1261938) is gratefully acknowledged.

■ REFERENCES

(1) Strebhardt, K.; Ullrich, A. *Nat. Rev. Cancer* **2008**, *8*, 473−480.
(2) Wilson, M. W.; Kerlan, R. K.; Fidelman, N. A.; Venook, A. P.; LaBerge, J. M.; Koda, J.; Gordon, R. L. *Radiology* **2004**, *230*, 287−293.
(3) Lubbe, A. S.; Bergemann, C.; Riess, H.; Schriever, F.; Reichardt, P.; Possinger, K.; Matthias, M.; Dorken, B.; Herrmann, F.; Gurtler, R.; Hohenberger, P.; Haas, N.; Sohr, R.; Sander, B.; Lemke, A. J.; Ohlendorf, D.; Huhnt, W.; Huhn, D.; Lübbe, A. S.; Dörken, B.; Gürtler, R. *Cancer Res.* **1996**, *56*, 4686−4693.
(4) Pouponneau, P.; Leroux, J.-C.; Soulez, G.; Gaboury, L.; Martel, S. *Biomaterials* **2011**, *32*, 3481−3486.
(5) Krukemeyer, M. G.; Krenn, V.; Jakobs, M.; Wagner, W. *J. Surg Res.* **2012**, *175*, 35−43.
(6) Liu, H.-L.; Hua, M.-Y.; Yang, H.-W.; Huang, C.-Y.; Chu, P.-C.; Wu, J.-S.; Tseng, I.-C.; Wang, J.-J.; Yen, T.-C.; Chen, P.-Y.; Wei, K.-C. *Proc. Natl. Acad. Sci. U.S.A.* **2010**, *107*, 15205−15210.
(7) Raut, S. L.; Kirthivasan, B.; Bommana, M. M.; Squillante, E.; Sadoqi, M. *Nanotechnology* **2010**, *21*, 395102.
(8) Koda, J.; Venook, A.; Walser, E.; Goodwin, S. *Eur. J. Cancer* **2002**, *38*, S18−S18.
(9) McBain, S. C.; Yiu, H. H. P.; Dobson, J. *Int. J. Nanomed.* **2008**, *3*, 169−180.
(10) Lemke, A. J.; von Pilsach, M. I. S.; Lubbe, A.; Bergemann, C.; Riess, H.; Felix, R. *Eur. Radiol.* **2004**, *14*, 1949−1955.
(11) Lemke, A.; Sander, B.; Luebbe, A.; Riess, H.; Hosten, N.; Felix, R. *Radiology* **1996**, *201*, 1421−1421.
(12) Pouponneau, P.; Leroux, J.-C.; Martel, S. *Biomaterials* **2009**, *30*, 6327−6332.
(13) Forbes, Z. G.; Yellen, B. B.; Halverson, D. S.; Fridman, G.; Barbee, K. A.; Friedman, G. *IEEE Trans. Biomed. Eng.* **2008**, *55*, 643−649.

dx.doi.org/10.1021/nl503654t | *Nano Lett.* XXXX, XXX, XXX−XXX

(14) Fernández-Pacheco, R.; Marquina, C.; Gabriel Valdivia, J.; Gutiérrez, M.; Soledad Romero, M.; Cornudella, R.; Laborda, A.; Viloria, A.; Higuera, T.; García, A.; de Jalón, J. A. G.; Ricardo Ibarra, M. *J. Magn. Magn. Mater.* **2007**, *311*, 318−322.
(15) Yanai, A.; Häfeli, U. O.; Metcalfe, A. L.; Soema, P.; Addo, L.; Gregory-Evans, C. Y.; Po, K.; Shan, X.; Moritz, O. L.; Gregory-Evans, K. *Cell Transplant.* **2012**, *21*, 1137−1148.
(16) Lübbe, a S.; Alexiou, C.; Bergemann, C.; Lubbe, A. S. *J. Surg. Res.* **2001**, *95*, 200−206.
(17) Polyak, B.; Fishbein, I.; Chorny, M.; Alferiev, I.; Williams, D.; Yellen, B.; Friedman, G.; Levy, R. J. *Proc. Natl. Acad. Sci. U.S.A.* **2008**, *105*, 698−703.
(18) Pislaru, S. V.; Harbuzariu, A.; Gulati, R.; Witt, T.; Sandhu, N. P.; Simari, R. D.; Sandhu, G. S. *J. Am. Coll. Cardiol.* **2006**, *48*, 1839−1845.
(19) Dobson, J. *Nanomedicine* **2006**, *1*, 31−37.
(20) Shapiro, B. *J. Magn. Magn. Mater.* **2009**, *321*, 1594.
(21) Hayden, M. E.; Hafeli, U. O. *J. Phys.: Condens. Matter* **2006**, *18*, S2877−S2891.
(22) Cao, Q.; Han, X.; Li, L. *J. Magn. Magn. Mater.* **2011**, *323*, 1919−1924.
(23) Schuerle, S.; Erni, S.; Flink, M.; Kratochvil, B. E.; Nelson, B. J. *IEEE Trans. Magn.* **2013**, *49*, 321−330.
(24) Brandt, E. H. *Science* **1989**, *243*, 349−355.
(25) Geim, A. K.; Simon, M. D.; Boamfa, M. I.; Heflinger, L. O. *Nature* **1999**, *400*, 323−324.
(26) Earnshaw, S. *Trans. Cambridge Philos. Soc.* **1842**, *7*, 97−112.
(27) Nacev, A.; Komaee, A.; Sarwar, A.; Probst, R.; Kim, S. H. S.; Emmert-Buck, M.; Shapiro, B. *IEEE Control Syst.* **2012**, *32*, 32−74.
(28) Weinberg, I. N.; Stepanov, P. Y.; Fricke, S. T.; Probst, R.; Urdaneta, M.; Warnow, D.; Sanders, H.; Glidden, S. C.; McMillan, A.; Starewicz, P. M.; Reilly, J. P. *Med. Phys.* **2012**, *39*, 2578−2583.
(29) Pankhurst, Q. A.; Connolly, J.; Jones, S. K.; Dobson, J. *J. Phys. D: Appl. Phys.* **2003**, *36*, R167.
(30) Feynman, R. P.; Leighton, R. B.; Sands, M. *The Feynman Lectures on Physics*; Addison-Wesley Publishing Company: Boston, 1964; Chapters 13 and 18, Vol. 2.
(31) Zborowski, M. In *Scientific and Clinical Applications of Magnetic Carriers SE-15*; Häfeli, U., Schütt, W., Teller, J., Zborowski, M., Eds.; Springer: New York, 1997; pp 205−231.
(32) Salem, A. K.; Searson, P. C.; Leong, K. W. *Nat. Mater.* **2003**, *2*, 668−671.
(33) Babincova, M.; Babinec, P.; Bergemann, C. *Zeit. Naturforsch. C-a: J. Biosci.* **2001**, *56*, 909−911.
(34) Polyak, B.; Friedman, G. *Expert Opin. Drug Delivery* **2009**, *6*, 53−70.
(35) Nacev, A.; Beni, C.; Bruno, O.; Shapiro, B. *Nanomed. London Engl.* **2010**, *5*, 1459−1466.
(36) Gleich, B.; Weizenecker, J. J. *Nature* **2005**, *435*, 1214−1217.
(37) Pankhurst, Q. A.; Thanh, N. T. K.; Jones, S. K.; Dobson, J. *J. Phys. D: Appl. Phys.* **2009**, *42*, 224001.
(38) Blums, E.; Cebers, A.; Maiorov, M. *Magnetic Fluids*; Walter de Gruyter & Co: Berlin, Germany, 1997; Chapters 1 and 5.
(39) Metzger, R. M.; Konovalov, V. V.; Zangari, G.; Benakli, M.; Doyle, W. D. *IEEE Trans. Magn.* **2000**, *36*, 30−35.
(40) Frka-Petesic, B.; Erglis, K.; Berret, J. F.; Cebers, A.; Dupuis, V.; Fresnais, J.; Sandre, O.; Perzynski, R. *J. Magn. Magn. Mater.* **2011**, *323*, 1309−1313.

Dynamic Inversion Enables External Magnets to Concentrate Ferromagnetic Rods to a Central Target

Authors: A. Nacev[1*], I. N. Weinberg[1], P.Y. Stepanov[1], S. Kupfer[1], L.O. Mair[1], M. G. Urdaneta[1], M. Shimoji[1], S.T. Fricke[2], B. Shapiro[3]

Affiliations:

[1]Weinberg Medical Physics LLC, Bethesda, Maryland.

[2]Children's National Medical Center, Washington DC

[3]Fischell Department of Bioengineering and the Institute for Systems Research, University of Maryland, College Park, Maryland.

*Correspondence to: alek@nacev.me

Supporting Information

Materials and Methods

As mentioned in the main text, two experimental systems were developed: a one-dimensional system capable of repelling rods in a single direction, and a two-dimensional system capable of repelling rods in four directions. The one-dimensional system was used for verification of the ability of the dynamic magnetic inversion technique to invert the magnetic potential energy surface and therefore push the rods. The two-dimensional system was to demonstrate the ability of the dynamic magnetic inversion technique to concentrate and focus rods to a central target.

1-D System: To verify the dynamics of repelled rods, we first created a one-dimensional magnet system that was able to repel and image ferromagnetic rods. This one-dimensional (1-D) push system used cobalt rods (that were 200 μm long and 200 nm in diameter from PlasmaChem GmbH, Cat. Nr. PL-CoW200) submerged in water and held within a glass tube. Around this glass tube, we wound two sets of coils: the polarizing and gradient coils (see Fig. S1A). When the polarizing coil was fired, a uniform magnetic field was produced within the 3 mm wide sample region. When the polarizing coil acted alone, the uniform field oriented the particles along the direction of the polarizing magnetic field. Once the polarizing coil was deactivated and the gradient coil was fired (Fig. S1B), a non-uniform magnetic field was created that was stronger towards the left side of the sample region, and the particles moved to the right (Fig. S1C), at a speed of 19 microns/second. When the gradient coil acted alone (i.e., without a prior polarizing pulse), the particles moved to the left (i.e., toward the gradient coil).

The 1-D push system has the following specifics: The polarizing coil consisted of two 1.7 cm wide segments of 100 turns of 30 American wire gauge magnet wire (RadioShack 278-1345) wrapped around a 6 mm diameter tube. The gradient coil was also 100 turns of the same magnet wire wound on-top of one half of the polarizing coils. Two high-power pulse generators (Velonex model 360) provided power to each coil at a maximum voltage of 2.5 kV and 11 A of current. Fig. S2A details the circuit diagram for the connection of the high-power pulse generator to the gradient and polarizing coils. A signal generator (BNC model 500B) externally triggered each pulse generator allowing for the pulse duration to be varied between 1 and 1000 μs with a 1% duty cycle. A USB digital microscope (Celestron model 44302-A) was used to gather a video of the rods' dynamics.

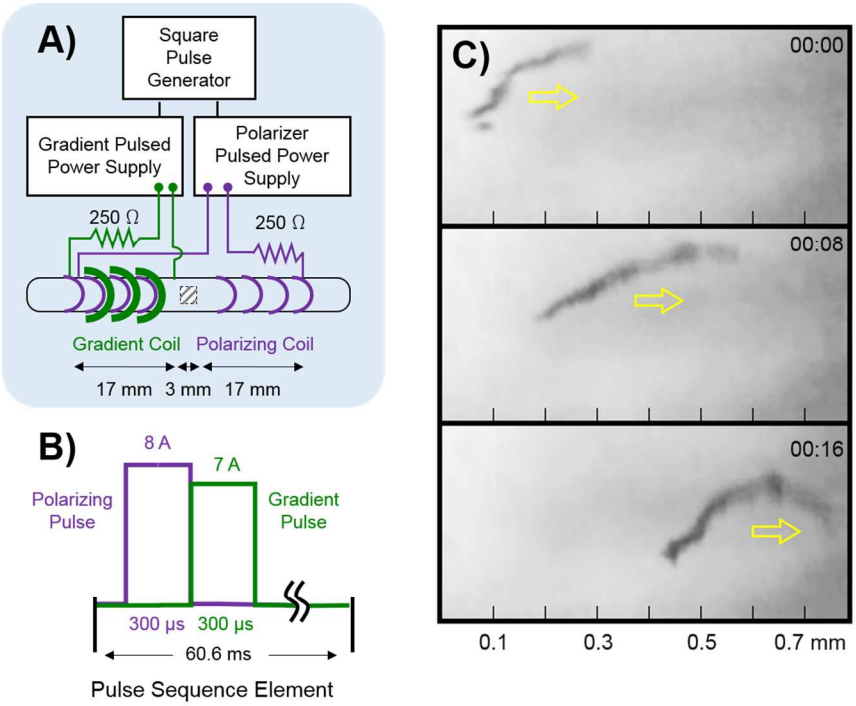

Fig. S1: Set-up schematic and results for 1-D dynamic magnetic inversion. A) Experimental set-up. The polarizing coils (purple) were two identical coils designed to create a uniform magnetic field within the sample area (hashed area in center). The gradient coil (green) was wound on only one side and produced a magnetic gradient within the sample region. B) Pulse sequence element used at 1% duty cycle that generated a push-force in the rightward direction acting upon the cobalt rods. C) Snapshots showing cobalt rods being pushed away from the gradient coil (located on left side of the image) at a speed of 19 µm/s ± 10 µm/s.

2-D System Specifics: The 2-D push experimental system has two pairs of polarizing coils for the *x*- and *y*-directions, and four gradient coils for +*x*, +*y*, -*x*, and -*y*. All coils surround a 25 mm x 25 mm sample region (see Fig. 5). To create a strong field intensity and gradient, the gradient coils were wound around a two centimeter diameter tube 120 times and placed next to the center region. The gradient coils were powered with the same high power pulse generator as for 1-D pushing, but with an additional module (Velonex V-1885) added that converted the generator's output to supply 400 V at 66 A. To create the uniform field, the polarizing coils were wound around a 5 cm square structure forty-four times. The pulse generator for the polarizing coils remained unchanged from the 1-D dynamic magnetic inversion case and provided a maximum current of 11 A. All coils used 28 American wire gauge magnet wire (TEMCo model MW0213).

A Matlab (from MathWorks) graphical user interface (GUI) created on a Windows computer was designed to control a Phidget microcontroller (Phidget Interface Kit 0/16/16, P/N 1012) and the same BNC signal generator as used for 1D magnetic inversion case. The Phidget board controlled the current path by flipping a series of high voltage relays (Gigavac GH1). By adjusting which relays were turned on, current would pass through a given coil, allowing for a particular movement axis to be selected (see Fig. S2B for the circuit diagram). The circuit diagram shows a representative schematic for one gradient coil. The system had four such circuits each connected to the common voltage source and ground as appropriate. A non-connected port was located on one relay of the gradient coils so that the mutual inductance on the inoperative gradient coils did not generate current within the coil and interfere with proper system function.

The GUI was able to completely dictate all aspects of the magnetic field except for the current level, which is controlled manually by adjusting the high-powered pulse generator voltage. Parameters controllable through the GUI included: polarizing magnetic field direction (+*x*, +*y*, -*x*, and -*y*), the active gradient coil, the direction of the gradient coil's magnetic field, the pulse sequence including the delay and width of each pulse, and the duty cycle of the pulse sequence. The GUI could then create a repulsion or attraction force in any of the four directions with any magnetic field alignment.

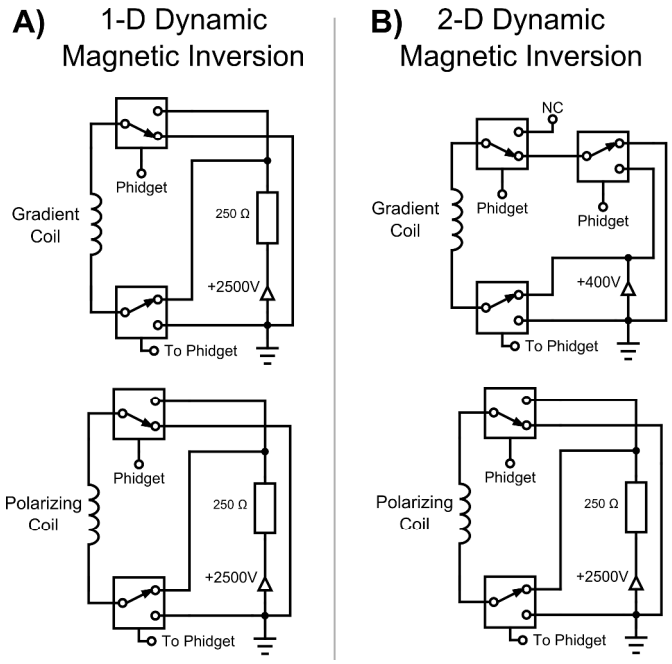

Fig. S2: Circuit diagram for the two experimental systems. A) Diagram for the gradient and polarizing coil relays used in the one-dimensional system. B) Diagram for the gradient and polarizing coil relays used in the two-dimensional system. Each relay is controlled by the Phidget controller.